Extension of the diffuse mismatch model for thermal boundary conductance between isotropic and anisotropic materials

John C. Duda,[1,a)] Justin L. Smoyer,[1,b)] Pamela M. Norris,[1,c)] and Patrick E. Hopkins[2,d)]
[1]*Department of Mechanical and Aerospace Engineering, University of Virginia, Charlottesville, Virginia 22904, USA*
[2]*Engineering Sciences Center, Sandia National Laboratories, Albuquerque, New Mexico 87185, USA*

(Received 24 June 2009; accepted 7 July 2009; published online 22 July 2009)

This model is an extension of the diffuse mismatch model (DMM), tailored to accurately predict thermal boundary conductance (h_{BD}) at interfaces where one material comprising the interface is characterized by high elastic anisotropy. Temperature-dependent specific heat is calculated with this vibrational model and compared to published values. Modifications to the DMM that incorporate the vibrational model are presented with predictions of h_{BD} at a metal-graphite interface. This model slightly underestimates experimental data, as expected, as the large acoustic mismatch between metals and graphite suggests inelastic scattering, something the DMM does not take into account.
 [DOI: 10.1063/1.3189087]

The ability to accurately predict thermal boundary conductance (h_{BD}) at interfaces is essential for the effective design of nanostructured devices, especially thermoelectrics,[1] and thermal interface materials.[2] One of the most widely implemented models for predicting h_{BD} is the diffuse mismatch model (DMM).[3] The DMM assumes that all incident phonons scatter diffusely and elastically at the interface between two materials. The probability of a phonon diffusely scattering across the interface is thus related only to the occupied density of states, the phonon group velocity, and the phonon energy on each side of the interface. The transmission coefficient from side 1 to side 2, which describes this probability, is given by

$$\zeta^{1\to 2}=\frac{\Sigma_j^3\int_0^{\omega_{D,j}}\hbar\omega\nu_{2,j}D(\omega,\nu_{2,j})f_{BE}d\omega}{\Sigma_j^3\int_0^{\omega_{D,j}}\hbar\omega\nu_{1,j}D(\omega,\nu_{1,j})f_{BE}d\omega+\Sigma_j^3\int_0^{\omega_{D,j}}\hbar\omega\nu_{2,j}D(\omega,\nu_{2,j})f_{BE}d\omega}, \tag{1}$$

where j is a particular polarization, ω is the phonon frequency, ω_D is the cutoff frequency, ν is the phonon group velocity, D is the density of states, and f_{BE} is the Bose–Einstein distribution. The elastic-only assumption included in the development of the DMM enforces that the upper limit for all integrals in Eq. (1) is the cutoff frequency of the material with the lower maximum vibrational frequency.

Simplifications to ζ can be made for interfaces between isotropic materials such that the expression appears in a more recognizable form. In the case where both materials that comprise the interface are three-dimensional isotropic Debye solids, where the three-dimensional Debye density of states is given by

$$D(\omega,\nu)=\frac{\omega^2}{2\pi^2\nu^3}, \tag{2}$$

integration over ω in Eq. (1) reduces ζ to

$$\zeta^{1\to 2}=\frac{\Sigma_j^3\nu_{2,j}^{-2}}{\Sigma_j^3\nu_{1,j}^{-2}+\Sigma_j^3\nu_{2,j}^{-2}}. \tag{3}$$

Integration over ω yields a frequency independent transmission coefficient. Still, the form of ζ as given by Eq. (3) is identical to the form presented by Swartz and Pohl.[3] Regardless of the formation of ζ, the DMM yields the following expression for h_{BD}:

$$h_{BD}^{1\to 2}=\frac{1}{4}\sum_j^3\int_0^{\omega_{D,j}}\zeta^{1\to 2}\hbar\omega\nu_{1,j}D(\omega,\nu_{1,j})\frac{\partial}{\partial T}f_{BE}d\omega. \tag{4}$$

While the DMM does provide an estimate of h_{BD} due to the difference in vibrational properties between the two materials that comprise an interface, it can largely over or underpredict experimentally determined values for many interfaces.[4,5] Modifications to the DMM have recently been developed to account for both mixing at interfaces,[6] as well as the contribution of inelastic scattering,[7] and both have shown a great improvement in overall accuracy of the model. This particular extension of the DMM accounts for interfaces between isotropic and highly anisotropic materials at elevated temperatures. Example calculations are given for metal-graphite interfaces.

a)Electronic mail: duda@virginia.edu.
b)Electronic mail: jls5ra@virginia.edu.
c)Electronic mail: pamela@virginia.edu.
d)Electronic mail: pehopki@sandia.gov.

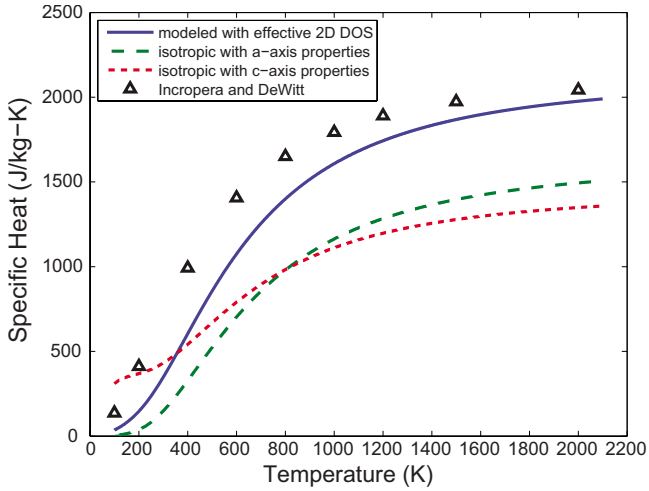

FIG. 1. (Color online) The specific heat of graphite as a function of temperature from 100 to 2000 K. The solid line is the value calculated using the effective density of states, D_{eff}, and the data points are published values (Ref. 8). As expected, this model underestimates the specific heat at lower temperatures as a result of ignoring interlayer vibrational modes. Still, it is evident that the model converges at the high-temperature limit.

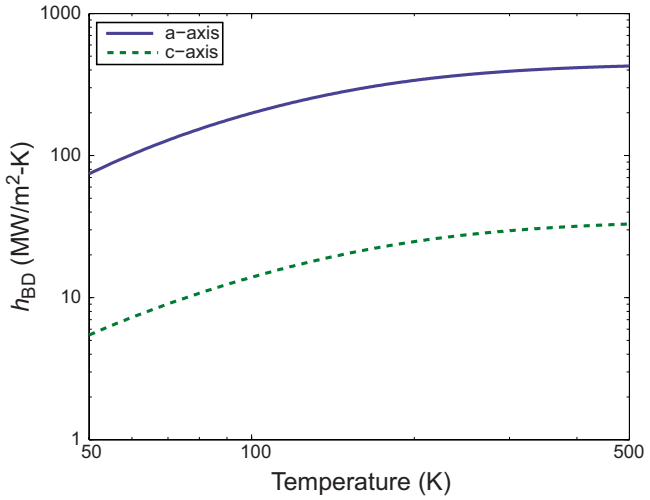

FIG. 2. (Color online) Predicted values of h_{BD} as a function of temperature from 50 to 500 K for the Al-graphite interface for both *a*- and *c*-axis graphite orientation. The predicted value for the *a*-axis orientation is over an order of magnitude higher than for the *c*-axis orientation for the entire temperature range.

Graphite is a highly anisotropic material, with *a*-axis (within the basal plane) and *c*-axis (perpendicular to the basal plane) thermal conductivities differing by nearly three orders of magnitude.[8] Any appropriate extension of the DMM must take this anisotropy into account. While other models have calculated h_{BD} at metal-graphite interfaces,[9] these calculations involve derivation and integration of the complex dispersion relations of graphite. However, for predictions of h_{BD} at metal-graphite interfaces at temperatures above cryogenic, the strong anisotropy of graphite allows for certain simplifying assumptions. Interlayer bonding in graphite is very weak and is often described as a van der Waals type interaction. The dispersion diagrams of graphite show that the acoustic interlayer vibrations that participate in thermal transport exist at frequencies below 3 THz, one to two orders of magnitude below the maximum longitudinal and transverse acoustic vibrational frequencies within the basal plane.[10] Additionally, studies looking at both graphite and carbon nanotubes have indicated that these interlayer vibrational modes saturate at temperatures above 50 K.[9,11]

Previous work has shown that as a result of this weak interlayer vibrational coupling, thermal conductivity of graphite can be determined by treating vibrations as a one- or two-dimensional phonon gas depending on orientation.[12] A similar reduction can be made when calculating other thermal properties. At elevated temperatures, the number of populated vibrational modes within the basal plane far exceeds the number of interlayer modes, as evident by the dispersion diagrams of graphite,[10,13] and the low temperature at which interlayer modes saturate.[9,11] Thus, the vibrational spectrum of each layer can be described by a two-dimensional Debye density of states,

$$D_{\text{2D}}(\omega,\nu) = \frac{\omega}{2\pi\nu^2}, \tag{5}$$

where ω is the frequency of a given phonon. To determine the density of states of an assembly of monolayers, this two-dimensional density of states must be scaled by N, or the number of monolayers per unit length. Thus, the effective density of states for the graphite bulk is given by

$$D_{\text{eff}}(\omega,\nu) = N\frac{\omega}{2\pi\nu^2} = \frac{\omega}{2\pi\nu^2}\frac{1}{d}, \tag{6}$$

where $d=3.35$ Å is the interlayer spacing for graphite.[14] Under this model, the single monolayer and the graphite bulk have the same maximum vibrational frequency; the only thing that differs is the number of available modes at each frequency. Note that three polarizations are considered because the assembly of two-dimensional subsystems creates a three-dimensional bulk system. While the vibrational modes of each monolayer or subsystem are not coupled, forces between the subsystems are responsible for the third polarization. The electronic contribution to thermal properties is not considered in the following derivation, as the number of effectively free electrons within the basal plane has been reported to be very low as compared to that of a typical metal ($n_{\text{eff}}=2.3\times10^{-4}$ electrons per atom).[15]

In order to validate this treatment of the vibrational modes, the specific heat of graphite was considered. Calculations of the specific heat of crystals with a basis greater than one must account for optical phonons via the Einstein model in addition to the acoustic phonon contribution using the Debye model. The formulation of the specific heat of Debye and Einstein solids is readily available in other references.[16] From examination of the vibrational spectrum and the dispersion diagrams for graphite,[10,13] the optical peaks occur at the acoustic cutoff frequencies for each polarization. The cutoff frequencies for each polarization are determined by

$$\omega_{\text{D},j} = \nu_j\sqrt{4\pi N}, \tag{7}$$

where N is the planar lattice-point density of a single monolayer. Using this cutoff frequency, the specific heat is calculated from 100 to 2000 K.

Figure 1 shows a comparison of specific heat calculated with the density of states given by Eq. (6), the specific heat calculated with the isotropic Debye density of states given by Eq. (2) using both *a*- and *c*-axis properties and published

values. The specific heat calculated using Eq. (6) matches the published data well at higher temperatures and converges to the high-temperature limit. The small discrepancy between calculated and reported values may lie within the assumption of the Einstein model that all optical phonons vibrate at the same frequency. Examination of the dispersion relationships reveals that this is not entirely accurate, but still provides a good estimate.[10] Since this model is concerned specifically with transport, a more accurate treatment of the optical phonons is not of primary interest since optical phonons do not greatly contribute to thermal transport. The calculated values of specific heat using the three-dimensional isotropic Debye density of states do not match the published data, demonstrating that an isotropic description of graphite is not accurate.

When using the effective density of states given by Eq. (6) to calculate both ζ and h_{BD}, one must be careful to consider the phonon group velocities for each polarization in the direction of transport, yet only use the in-plane phonon velocities when calculating the density of states. Again, if each graphite monolayer is treated as an independent two-dimensional subsystem, its vibrational states are dictated by its two-dimensional properties, or under the Debye approximation, the in-plane phonon group velocity. Thus, $\zeta^{1\to2}$, where heat flows from side 1, a metal film, to side 2, a graphite substrate, becomes

$$\zeta^{1\to2} = \frac{\Sigma_j^3 \int_0^{\omega_{D,j}} \hbar\omega \nu_{2,j} D_{\text{eff}}(\omega, \nu_{a,j}) f_{BE} d\omega}{\Sigma_j^3 \int_0^{\omega_{D,j}} \hbar\omega \nu_{2,j} D_{\text{eff}}(\omega, \nu_{a,j}) f_{BE} d\omega + \Sigma_j^3 \int_0^{\omega_{D,j}} \hbar\omega \nu_{1,j} D_{3D}(\omega, \nu_{1,j}) f_{BE} d\omega}, \tag{8}$$

at which point h_{BD} can be calculated by Eq. (4). Figure 2 shows h_{BD} as a function of temperature from 50 to 500 K for the Al-graphite interface for two different orientations of graphite. The predicted value for the *a*-axis orientation is over an order of magnitude higher than for the *c*-axis orientation for the entire temperature range. This result seems logical, both intuitively and conceptually, as the thermal conductivity, and hence, the phonon group velocity, is much higher in-plane compared to out-of-plane. The room temperature h_{BD} at the Al-graphite interface (*c*-axis) has been reported as 50 $\text{MW/m}^2\,\text{K}$.[17] The model-predicted value is 30 $\text{MW/m}^2\,\text{K}$, a 40% underprediction. This is to be expected, however, as the elastic-only assumption made by the DMM will significantly limit the number of phonons that can participate in transport at the interface. Still, the accuracy of this model is quite good when considering the order-of-magnitude error often associated with the DMM.[5]

Overall, the underlying physics of the graphite structure, as well as a comparison of predicted specific heat to published values, establishes the validity of the model when calculating thermal properties at elevated temperatures. An extension of the DMM employing this vibrational model has been presented, with applicability to predicting h_{BD} at interfaces between isotropic and highly anisotropic materials. Comparison between the predicted and experimental room temperature h_{BD} at an Al-graphite interface shows good agreement, and the underprediction is to be expected. This model can easily be extended to other anisotropic media where weak coupling between subsystems is present. Further experimental data will be required to evaluate the temperature range over which this model is valid.

The authors acknowledge the financial support of Office of Naval Research through a MURI grant (Grant No. N00014-07-1-0723). J.C.D is greatly appreciative for financial support from the National Science Foundation through the Graduate Research Fellowship Program. J.C.D. and J.L.S. would like to thank Dr. William Soffa from U.Va. for his meticulous instruction and helpful insight. P.E.H. is grateful for funding from the LDRD program office through the Sandia National Laboratories Harry S. Truman Fellowship. Sandia is a multiprogram laboratory operated by Sandia Corporation, a Lockheed-Martin Co., for the United States Department of Energy's National Nuclear Security Administration under Contract No. DE-AC04-94AL85000.

[1] L. W. da Silva and M. Kaviany, Int. J. Heat Mass Transfer **47**, 2417 (2004).
[2] T. Tong, Y. Zhao, L. Delzeit, A. Kashani, M. Meyyappan, and A. Majumdar, IEEE Trans. Compon. Packag. Technol. **30**, 92 (2007).
[3] E. T. Swartz and R. O. Pohl, Rev. Mod. Phys. **61**, 605 (1989).
[4] P. E. Hopkins, P. M. Norris, and R. J. Stevens, J. Heat Transfer **130**, 022401 (2008).
[5] P. M. Norris and P. E. Hopkins, J. Heat Transfer **131**, 043207 (2009).
[6] T. Beechem, S. Graham, P. Hopkins, and P. Norris, Appl. Phys. Lett. **90**, 054104 (2007).
[7] P. E. Hopkins and P. M. Norris, Nanoscale Microscale Thermophys. Eng. **11**, 247 (2007).
[8] F. P. Incropera and D. P. DeWitt, *Fundamentals of Heat and Mass Transfer*, 5th ed. (Wiley, New York, 2002).
[9] R. Prasher, Phys. Rev. B **77**, 075424 (2008).
[10] R. Nicklow, N. Wakabayashi, and H. G. Smith, Phys. Rev. B **5**, 4951 (1972).
[11] P. Kim and L. Shi, A. Majumdar, and P. L. McEuen, Phys. Rev. Lett. **87**, 215502 (2001).
[12] K. Sun, M. A. Stroscio, and M. Dutta, Superlattices Microstruct. **45**, 60 (2009).
[13] J. Maultzsch, S. Reich, C. Thomsen, H. Requardt, and P. Ordejon, Phys. Rev. Lett. **92**, 075501 (2004).
[14] Y. Baskin and L. Meyer, Phys. Rev. **100**, 544 (1955).
[15] P. R. Wallace, Phys. Rev. **71**, 622 (1947).
[16] C. Kittel, *Introduction to Solid State Physics*, 8th ed. (Wiley, New York, 2005).
[17] A. J. Schmidt, X. Chen, and G. Chen, Rev. Sci. Instrum. **79**, 114902 (2008).